

Ferroelectric Research: The Basic Fundamental Understanding

M.N.A. HALIF

*School of Microelectronic Engineering, Kolej Universiti Kejuruteraan Utara Malaysia (KUKUM)
Jalan Kangar-Arau, 02600 Jejawi, Perlis, MALAYSIA.*

ABSTRACT

This paper gives an overview of the basic theoretical aspect of ferroelectric materials. The basic theoretical concepts are described from the Landau free-energy density F in the first and second-order ferroelectric phase transitions in terms of free-energy expansion curves, hysteresis loop, and polarization reversal.

E-mail: *m.nazri@kukum.edu.my* ; Tel: +604-9798301, Fax: +604-9798305

Keyword (s): *Ferroelectrics; Landau theory; Phase Transition.*

GENERAL OVERVIEW

The permanent electric dipole moment possessed by all pyroelectric (polar) materials may, in certain cases, be oriented by the application of an electric field. Such materials are called ferroelectric (FE). Research on FE materials was started by Seignette from study of Rochelle salt ($\text{NaKC}_4\text{H}_4\text{O}_6\cdot 4\text{H}_2\text{O}$) in 1655 at Rochelle, France. In 1921, ferroelectricity was discovered by J. Valasek during an investigation of anomalous dielectric properties of Rochelle salt. It was the first major substance of FE. A second FE material KH_2PO_4 was not discovered until 1935 and it was followed by some of its isomorphs. Later, the phenomenological theory was introduced to give a deeper understanding of dielectric behavior, piezoelectric and strange elastic behavior in FE crystals. A basic macroscopic theory for FE materials, so called phase transitions theory for KH_2PO_4 has been developed¹. The third major substance, BaTiO_3 was reported by von Hippel A.² in 1944 and it had a high dielectric constant from 1000 to 3000 at room temperature³. Ref. 4 and 5 give details of the general properties of physics and historical perspective on discovery of ferroelectric respectively.

Later, the number of FE materials increased drastically due to the strong influence by researchers to explore and study FE materials and up to now there are more than 200 species of FE. The other example of FE materials are BaTiO_3 , PbTiO_3 , SrTiO_3 , LiNbO_3 , LiTaO_3 , lead zirconate titanate (PZT), lead lanthanum zirconate

titanate (PLZT) and relaxor FE like lead magnesium niobate (PMN) and BaMgF₄ (BMF). Table 1 in **Appendix A** gives some typical FE with critical temperature T_C and spontaneous polarization P_S .

In the next section, we will discuss some basic issues from theoretical background in terms of the Landau free energy expansion, hysteresis loop and polarization reversal. In the last section, we may summarize some important aspect of ferroelectric applications.

BASIC THEORETICAL BACKGROUND

Basically, we start with a brief account of theoretical background for bulk FE materials since these are the main points of reference to understand the behavior in different geometrical sizes: semi-infinite and thin film. One of the basic characteristic of FE materials is it can exist in two states of phase transitions: first and second-order phase transitions, respectively. These kinds of FE behavior are described using the Landau theory, a simple but powerful empirical thermodynamic theory by which the behavior of crystals at phase transitions can be described. It is based simply on a power series expansion of the free energy of the crystal with respect to one or a few prominent parameters distorting the symmetry of the crystal. With this theory, the thermodynamics of the crystal (free energy, entropy, heat capacity) can be directly linked to its structural state (volume, deviation from high symmetry, etc.), and both can be described as they change as a function of temperature or pressure. In the Landau-theory, the free-energy density F is expanded as a power series in the component of the polarization P . The free-energy density may be described by the Landau-Devonshire (LD) free-energy expansion⁵⁻¹¹ in the electrical polarization P

$$F(P, T) = F_0 + \alpha P^2 + \beta P^4 + \gamma P^6 \quad (1)$$

in the equilibrium state with $E = 0$ where $\alpha = A/2\epsilon_0^2$, $\beta = |B|/4\epsilon_0^2$, and $\gamma = C/6\epsilon_0^2$. F_0 is the free-energy density of the paraelectric (PE) phase ($P = 0$) at zero electric field. $A = a(T - T_0)$, with a representing inverse Curie constant and T_0 is the Curie temperature for bulk sample. A , B , and C are the dependent material parameters (see **Table 2 in Appendix A**). For first-order phase transition, $B < 0$ and $C > 0$, while for second-order, $B > 0$ and $C < 0$, and usually C is omitted. P is the order parameter in LD free-energy density expansion. The odd terms on the power series expansion often are not allowed because the energy of the system is symmetrical with respect to positive or negative distortion. The spontaneous polarization may be calculated from the minimization of F , thus

$$P = \pm \left[\frac{1}{3\gamma} \left(-\beta + \frac{1}{2} \sqrt{4\beta^2 - 6\gamma\alpha} \right) \right]^{1/2} \quad \text{and} \quad P = \sqrt{\frac{-\alpha}{4\beta}} \quad \text{for } \alpha < 0 \quad (2)$$

for first and second-order phase transitions, respectively.

Figure 1(a) and 1(b), below show the equilibrium free-energy curves versus polarization in various temperatures for first and second-order case, respectively in dimensionless form using conventional scaling¹⁰ to perform the universal result without any materials dependence. For the first-order case, there are various ranges of temperatures⁵⁻¹¹; t_{SCB} the supercooling temperature where the stable-state for FE phase and metastable state for PE phase t_{CB} the bulk critical thermodynamic temperature where the FE stable-state begins to change to become FE metastable state and is the starting point for stable-state for PE. Here, the red dot points for FE and PE are at the same free-energy. $t < t_{CB}$ are considered as pure FE phase. At the superheating temperature t_{SHB} , FE is in the metastable-state while PE in stable-state and the phase transitions temperature is t_2 or so-called upper limit temperature and the temperature above this point called the pure PE phase. At $t_{SHB} < t < t_2$, these ranges are for the field-induced FE phase, where external electric fields are needed to be in the FE phase. For the second-order case, $t < t_0$ (t_0 : transitions temperature) are the pure FE phases where the red dots show the stable-state for FE phase. Lines and Glass⁵ gives a detail discussion of the FE free-energy behavior.

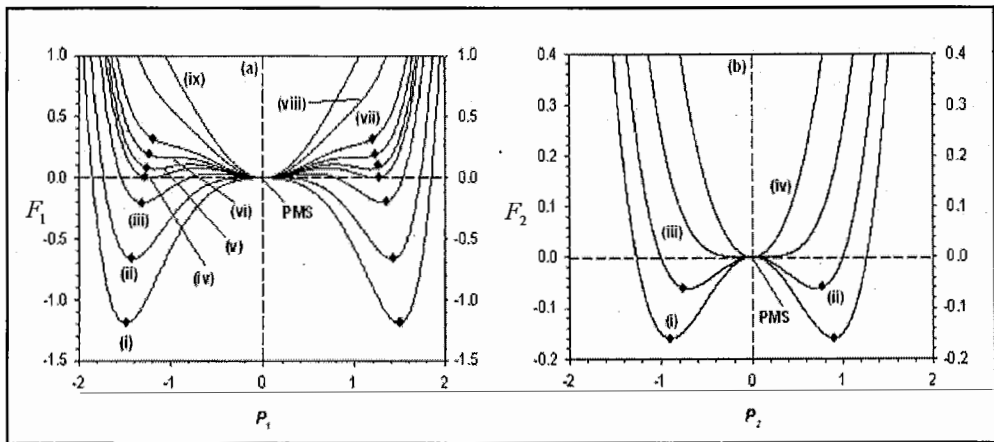


Figure 1: The equilibrium state of the Landau-Devonshire (LD) free-energy density curves for (a) first-order phase transition and (b) second-order phase transitions at various temperatures t in dimensionless unit. F_1 and F_2 refers to the Landau free-energy for the first and second-order phase transition, respectively. From Fig. 1(a); (i) $t = -0.5$ ($t < t_{SCB}$), (ii) $t = 0$, ($t = t_{SCB}$), (iii) $t = 0.5$ ($t_{SCB} < t < t_{CB}$), (iv) $t = 0.75$ ($t = t_{CB}$), (v) $t = 0.85$ ($t_{CB} < t < t_{SHB}$), (vi) $t = 1$, ($t = t_{SHB}$), (vii) $t = 1.2$ ($t_{SHB} < t < t_2$), (viii) $t = 1.8$ ($t = t_2$) and (ix) $t = 2.5$ ($t > t_2$). While for Fig. 1(b), (i) $t_r = 0.2$, (ii) $t_r = 0.5$, (iii) $t_r = 1.0$ ($t_r = t_0$), and (iv) $t_r = 2.0$ ($t_r > t_0$), where t_{SCB} : supercooling bulk temperature, t_{CB} : critical bulk temperature, t_{SHB} : superheating bulk temperature, t_2 : upper-limit temperature, and t_0 : phase transitions temperature for second-order case. The black dots have shown the FE stable-state points towards FE metastable points and the PMS (paraelectric (PE) metastable) points towards stable-state PE point when temperatures are increased.

From the free-energy expansion of (1) with $E \neq 0$, by taking first derivative, then

$$\frac{dF}{dP} = E = 2\alpha P + 4\beta P^3 + 6\gamma P^5 \quad (3)$$

where we may evaluate the discontinuous and continuous behavior of polarization P and temperature T at the minimum state ($dF/dP = 0$) as illustrated in Fig. 2. Section with the negative slope, $dP/dT < 0$ are thermodynamically stable. Eq. (2) above is also called the equation for the extrema on the LD free-energy curve (Fig. 1) and it gives the dielectric equation of state ($dF/dP = E$), which is polarization P versus electric field E , namely hysteresis loop are shown in Fig. 3(a) and 3(b) for first and second-order phase transitions, respectively. From the extrema of (3) the quadratic equation of P^2 for first and second-order case may be written as

$$P_c^2 = \frac{1}{5\gamma} \left[-\beta \pm \frac{1}{2} \sqrt{9\beta^2 - 15\gamma\alpha} \right] \text{ and } P_c^2 = \frac{-\alpha}{6\beta} \text{ for } \alpha < 0 \quad (4)$$

respectively, and by substituting (4) into (3), gives

$$E_c = \pm P_c \left[2\alpha - \frac{2\beta}{5} (2\beta + 3) \pm \left(\frac{\beta}{\gamma} - 1 \right) \sqrt{9\beta^2 - 15\gamma\alpha} \right] \text{ and } E_c = \pm \frac{4\alpha}{3} P_c \quad (5)$$

are called the comprehensive coercive electric field for the first and second-order phase transitions, respectively. The coercive field is defined as the effectiveness of electric field required to reestablish the polarization into zero. $E \geq E_c$ are the foremost condition for spontaneous polarization to repeal their state. The hysteresis function of $P(E)$ are shown in Fig. 3. The curves illustrated the bistable nature of polarization; the polarization reversal occurred only when the magnitude of E exceeded the coercive field E_c at the turning points in the function of $P(E)$. Figure 4(a) and 4(b) show the LD free-energy for non-equilibrium state, so called the switching behavior of polarization for first and second-order phase transitions, respectively. The graphs represented the two states of temperatures at pure FE phase. The increase of positive electric field towards $E \geq E_c$ gives the shifting phenomena to the FE stable-state represented by red dots. As mentioned earlier, this phenomenon shows that permanent electric dipole (polarization) may be oriented by application of electric field and the so-called switching. There are many experimental observation to study the switching behavior for FE materials, for example Merz¹¹ using optical method to observe the BaTiO₃ domain structure, recording the motion of 90° and 180° domain walls in single crystal BaTiO₃ thin film using TEM. Shur et al.¹² found that the domain dynamics essentially depend on applied electric field. The reversal process has often been analyzed using a method based upon Kolmogorov-Avrami (KA) theory¹³, which was originally a model of crystal growth¹⁴.

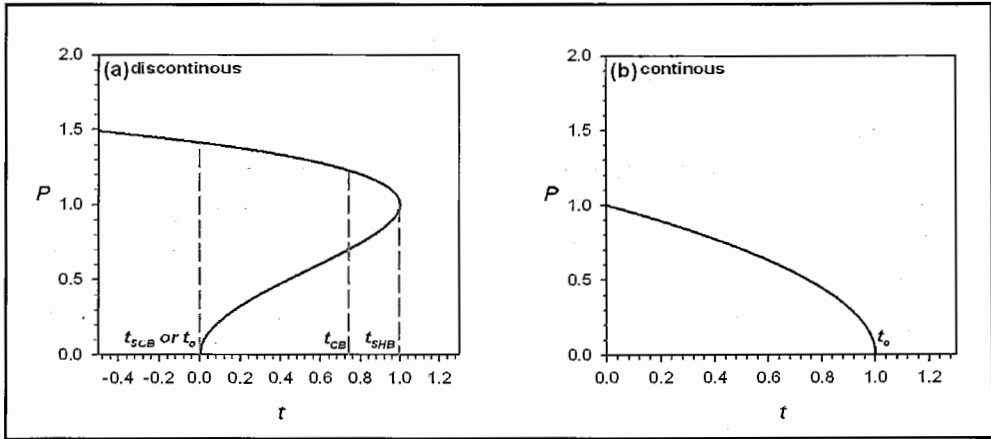


Figure 2: The dependence of temperature t for the order parameter, polarization P , for (a) First-Order and (b) Second-Order phase transition. There are three major ranges of temperature for the first-order case, represented by vertical dashes-red-line: the bulk supercooling t_{SCB} or $t_0 = 0$, bulk critical thermodynamic $t_{CB} = 0.75$, and bulk superheating $t_{SHB} = 1$, while for second-order case, $t_0 = 1$ represented the transition temperature.

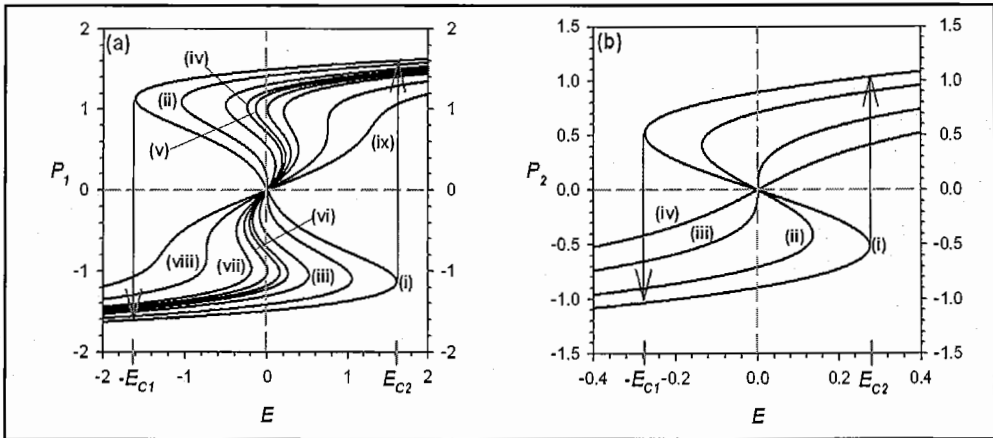


Figure 3: Hysteresis loop of polarization P versus E for (i) first-order case, and (ii) second-order case, respectively. The temperatures for (a) and (b) are the same as in Fig. 1. The vertical arrows show the external hysteresis loop and coercive fields E_{C1} and E_{C2} for one example of temperature $t = -0.5$ and $t_r = 0.2$ for first and second-order, respectively.

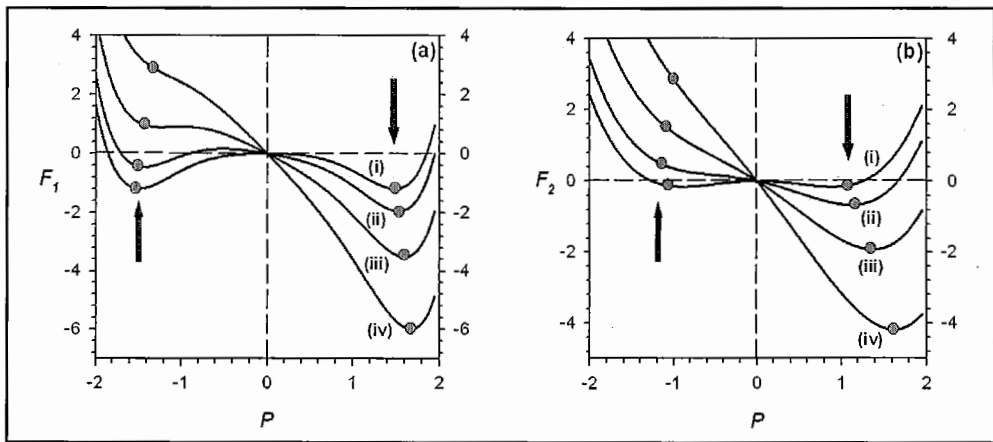


Figure 4: Switching behavior of the FE free-energy expansion at pure FE phase with (a) first-order at $t = -0.5$, and (b) second-order at $t_r = 0.2$, respectively. The effect of positive external electric field E ; (i) $E = 0$ (equilibrium state) (ii) $E = 0.5$ (iii) $E = 1.5$ and (iv) $E = 3$. The black dots are shown the changing of polarization P with the increasing of E from negative to positive shown by vertical arrows.

CONCLUSION

Figure 1 – 4 give the basic overview of FE behavior in terms of basic fundamental understanding. Currently, a lot of research has been done based on theoretical investigation to support the experimental investigation¹⁵ towards developing good and productive future electronic devices. The biggest usage of FE ceramics has been in the areas such as dielectric ceramics for capacitor applications, infrared movement detectors for auto-focusing cameras¹⁶, FE thin film for non-volatile memories, piezoelectric materials, medical ultrasound imaging and actuators, and electro-optic materials for data storage and display^{17,18}. In recent years, ferroelectric materials and thin films have attracted much attention and exhibited potential in many important applications such as dynamic random access memories (DRAMs), non-volatile ferroelectric random access memories, micro-armours and infrared sensors. At present, the ferroelectric materials that suitable for these devices are $\text{Pb}(\text{Zr},\text{Ti})\text{O}_3$ (PZT) systems, $\text{SrBi}_2\text{Ta}_2\text{O}_9$ (SBT) systems, $\text{Bi}_4\text{Ti}_3\text{O}_{12}$ (BIT) systems and BaTiO_3 (BT) systems are studied with a great deal of interest. In these ferroelectric materials, $\text{BaTi}_{0.91}(\text{Hf}_{0.5}\text{Zr}_{0.5})_{0.09}\text{O}_3$ (BTHZ-9), one of the BT systems which has several advantages such as an extremely low coercive field, a high remnant polarization, better mechanical strength and small deviation in composition, could have a strong potential application for ferroelectric thin film devices.

Ferroelectric Random Access Memory (FRAM) is non-volatile memories and is one of the examples of the successful ferroelectric-semiconductor research and it offer a unique set of features relative to other semiconductor technologies. Non-

volatile memories do not lose their contents when power is removed. FRAM also offers features consistent with a RAM technology, but it is non-volatile like ROM technology. FRAM bridges the gap between the two categories and creates something completely new, the so called non-volatile RAM. In general, the use of FE in thin film form has advantages on reduced size, weight and, especially, such devices were non-volatility (memory is not lost if power is interrupted), low power consumption (voltage-driven devices), radiation hardness, overall robustness and high speed¹⁹. For the last three decades, floating-gate memories have been the dominant class of non-volatile memories in applications ranging from personal computers to consumer electronics.

FUTURE WORK

While the indirect applications of FE mentioned above may continue to be more important in electronics research area, the more recent direct applications are likely to become more important because of the link to computer memories and data transfer. Since the size-effects become more important in the area of nanotechnology thus there is still a lot of work to be done in this area. Theoretical study of the behavior of FIR waves and the oscillatory dynamical switching properties in the asymmetrical FE films is also one of the focusses. On the other hand, the future work also focusses on some experimental study of deposition the FE materials, i.e BaTiO₃, PbTiO₃, and PZT on silicon. The author is pursuing these matters and hopes to publish the results soon.

ACKNOWLEDGEMENTS

This work was supported by KUKUM fundamental research grant: 9003-00011

REFERENCES

1. Slater J.C. (1941). *J. Chem. Phys.* 9:16.
2. Von Hippel A., Breckenridge R.G., Chesley F.G., and Tisza L. (1946). *Ind.Eng Chem.* 38:1097.
3. Wul B. and Goldman I.M. (1946). *Compt. Rend. Acad. Sci. U.S.S.R.* 51: 21.
4. Webb J.F. (2003). *Science Progress.* 86: 203.
5. Lines M.E., and Glass A.M. (2001). *Principles and Applications of Ferroelectrics and Related Materials*, Clarendon Press, New Edition.Oxford.
6. Blinc R., and Zeks B. (1974). *Soft Mode in Ferroelectrics and Antiferroelectrics.* Amsterdam: North-Holland.

7. Mitsui T., Tatsuzaki I., and Nukamira E. (1974). *An Introduction to The Physics of Ferroelectrics*. New York: Gordon and Breach.
8. Strukov B.A., and Levanyuk A.P. (1998). *Ferroelectric Phenomena in Crystal*. Berlin: Springer-Verlag.
9. Fatuzzo E. and Merz W.J. (1967). *Ferroelectricity*. Amsterdam: North-Holland.
10. Tan E.K., Junaidah Osman, and Tilley D.R. (2001). *Phys. Stat. Sol. (b)*, 228: 765.
11. Känzig W. (1957). *Ferroelectrics and Antiferroelectrics*. New York: Academic Press .
12. Merz W. (1954). *Phys. Rev.* 95: 3.
13. Shur V. Ya, Gruverman A.L., Ponomarev N. Yu, Rumyantsev E.L., Tonkachyova N.A. (1992). *Integrated Ferroelectrics*. 2: 51.
14. Klomogorov A.K. (1937). *Izv. Akad. Nauk Math.* 3: 355.
15. Avrami M. (1941). *J. Chem. Phys.* 9: 177.
16. Palkar V.R., Purandare S.C., and Pinto R. (1999). *J. Phys. D: Appl. Phys.* 32: R1-R18.
17. Xu Y. (1991). *Ferroelectric Materials and Their Applications*. North-Holland, Amsterdam.
18. Daglish M. and Kemmitt T. (2000). *IPENZ Transactions*. 27: 21.
19. Scott J.F., and Paz de Araujo C.A. (1989). *Science*. 246: 400.
20. Subarao E.C. (1973). *Ferroelectrics*. 5: 267.
21. Wang Y.G., Zhong W.L., and Zhang P.L. (1994). *Solid State Commun.* 92: 519.

APPENDIX A

Table 1: Some typical ferroelectric materials^{4,20}.

Type	Formula	T_C (K)	P_s in $\mu\text{C cm}^{-2}$
Perovskite	BaTiO ₃	408	26.0
	KNbO ₃	708	30.0
	PbTiO ₃	765	>50
	LiNbO ₃	1480	71.0
KDP	KH ₂ PO ₄	123	4.75
	KD ₂ PO ₄	213	4.93
	RbH ₂ PO ₄	147	5.6
	KH ₂ AsO ₄	97	5.0

Table 2: Landau free-energy parameters²¹ (mks unit).

FE materials	Bulk Curie Temp. $T_{C\infty}$ (K)	Bulk Curie-Weiss Temp. $T_{0\infty}$ (K)	Curie constant ($10^5 K$)	a (10^{-5}) (K^{-1})	B (10^{-13}) ($\text{ms}^2\text{kg}^{-1}$)	C (10^{-22}) ($\text{m}^2\text{s}^4\text{kg}^{-2}$)	D (10^{-21}) (m^2)
BaTiO ₃	408	391	1.7	5.891	-2.788	1.867	1005
PbTiO ₃	765	722	4.1	0.247	-1.267	2.925	3.980